

# Quantifying ligand–cell interactions and determination of the surface concentrations of ligands on hydrogel films: The measurement challenge

Cite as: Biointerphases 10, 021007 (2015); <https://doi.org/10.1116/1.4919015>

Submitted: 01 February 2015 • Accepted: 09 April 2015 • Published Online: 08 May 2015

Meike V. Beer, Kathrin Hahn, Sylvia Diederichs, et al.



View Online



Export Citation



CrossMark

## ARTICLES YOU MAY BE INTERESTED IN

[Orientation and characterization of immobilized antibodies for improved immunoassays \(Review\)](#)

Biointerphases 12, 02D301 (2017); <https://doi.org/10.1116/1.4978435>

[Dielectric barrier discharge plasma treatment of ultrahigh molecular weight polyethylene in different discharge atmospheres at medium pressure: A cell-biomaterial interface study](#)

Biointerphases 10, 029502 (2015); <https://doi.org/10.1116/1.4907755>

[Tribological changes in the articular cartilage of a human femoral head with avascular necrosis](#)

Biointerphases 10, 021004 (2015); <https://doi.org/10.1116/1.4919020>



**Biointerphases**  
A Journal of Biomaterials and Biological Interfaces

SPECIAL TOPIC

Polymeric Biointerfaces — A Collection  
in celebration of Nicholas D. Spencer's career



Submit Today!

# Quantifying ligand–cell interactions and determination of the surface concentrations of ligands on hydrogel films: The measurement challenge

Meike V. Beer and Kathrin Hahn

*Department of Functional Materials in Medicine and Dentistry, University of Würzburg, Pleicherwall 2, 97070 Würzburg, Germany*

Sylvia Diederichs, Marlies Fabry, and Smriti Singh

*DWI Leibniz Institute for Interactive Materials Research and Institute of Technical and Macromolecular Chemistry, RWTH Aachen University, Forckenbeckstr. 50, 52056 Aachen, Germany*

Steve J. Spencer

*National Physical Laboratory, Hampton Road, Teddington, Middlesex TW11 0LW, England*

Jochen Salber

*Clinic of Surgery, Knappschafts-Hospital GmbH, University Hospital of the Ruhr-University Bochum, 44892 Bochum, Germany*

Martin Möller

*DWI Leibniz Institute for Interactive Materials Research and Institute of Technical and Macromolecular Chemistry, RWTH Aachen University, Forckenbeckstr. 50, 52056 Aachen, Germany*

Alexander G. Shard

*National Physical Laboratory, Hampton Road, Teddington, Middlesex TW11 0LW, England*

Jürgen Groll<sup>a)</sup>

*Department of Functional Materials in Medicine and Dentistry, University of Würzburg, Pleicherwall 2, 97070 Würzburg, Germany*

(Received 1 February 2015; accepted 9 April 2015; published 8 May 2015)

Hydrogels are extensively studied for biomaterials application as they provide water swollen noninteracting matrices in which specific binding motifs and enzyme-sensitive degradation sites can be incorporated to tailor cell adhesion, proliferation, and migration. Hydrogels also serve as excellent basis for surface modification of biomaterials where interfacial characteristics are decisive for implant success or failure. However, the three-dimensional nature of hydrogels makes it hard to distinguish between the bioactive ligand density at the hydrogel-cell interface that is able to interact with cells and the ligands that are immobilized inside the hydrogel and not accessible for cells. Here, the authors compare x-ray photoelectron spectrometry (XPS), time-of-flight secondary ion mass spectrometry (ToF-SIMS), enzyme linked immunosorbent assay (ELISA), and the correlation with quantitative cell adhesion using primary human dermal fibroblasts (HDF) to gain insight into ligand distribution. The authors show that although XPS provides the most useful quantitative analysis, it lacks the sensitivity to measure biologically meaningful concentrations of ligands. However, ToF-SIMS is able to access this range provided that there are clearly distinguishable secondary ions and a calibration method is found. Detection by ELISA appears to be sensitive to the ligand density on the surface that is necessary to mediate cell adhesion, but the upper limit of detection coincides closely with the minimal ligand spacing required to support cell proliferation. Radioactive measurements and ELISAs were performed on amine reactive well plates as true 2D surfaces to estimate the ligand density necessary to allow cell adhesion onto hydrogel films. Optimal ligand spacing for HDF adhesion and proliferation on ultrathin hydrogel films was determined as  $6.5 \pm 1.5$  nm. © 2015 Author(s). All article content, except where otherwise noted, is licensed under a Creative Commons Attribution 3.0 Unported License. [<http://dx.doi.org/10.1116/1.4919015>]

## I. INTRODUCTION

Biomaterials can act as diagnostic materials in contact with body fluids, or as temporary or permanent substitute for organs, parts of organs or body structures, which are

destroyed or restricted in terms of function. In the latter application, foreign body reactions are still a significant complication across materials classes that usually occur within the first 2–3 weeks of implantation.<sup>1</sup> The initial compatibility of biomaterials is mainly determined by the materials' interface<sup>2</sup> and highly depends on the inhibition of unspecific protein adsorption as a first step leading to inflammation.<sup>3,4</sup> In order to allow interaction of the materials with

<sup>a)</sup> Author to whom correspondence should be addressed; electronic mail: [juergen.groll@fmz.uni-wuerzburg.de](mailto:juergen.groll@fmz.uni-wuerzburg.de)

the surrounding tissue, a useful strategy is to present specific interacting ligands to allow specific and desirable interactions of proteins or cells with the otherwise inert surfaces.

Biosensors and modern biomaterials are designed to actively interact with their environment, either through their stiffness, structure/morphology and/or bioactivation. For the latter, a variety of coating systems have been developed. The most important classes of systems are self-assembled-monolayers,<sup>5–8</sup> grafting from polymer brushes,<sup>9–12</sup> and hydrogel layers.<sup>13,14</sup> Self-assembled monolayers and grafting from brushes are ultrathin and well defined, so that introduction of functional groups such as cell adhesion peptides can be controlled precisely.<sup>15,16</sup> In contrast, hydrogel films are three dimensionally cross-linked polymer networks with thicknesses ranging from few nanometers to several micrometers. Embedded functional groups may thus be located near the surface or in the volume of the gels. In the latter scenario, cell adhesion molecules (CAMs) are not accessible for cells and will thus not support cell adhesion. Hence, one key parameter for characterization of these materials is the quantification of surface ligand density. However, although many hydrogel systems have been functionalized with ligands such as cell adhesion mediating peptides and proteins,<sup>17</sup> the quantification of the ligand concentration at the hydrogel interface that is decisive for cell adhesion is often disregarded.

Multiple quantification methods such as radiolabeling,<sup>18–20</sup> x-ray photoelectron spectrometry (XPS),<sup>21</sup> time-of-flight secondary ion mass spectrometry (ToF-SIMS),<sup>20,22,23</sup> enzyme linked immunosorbent assay (ELISA),<sup>24</sup> quartz crystal microbalance (QCM),<sup>25</sup> ellipsometry,<sup>19</sup> surface plasmon resonance (SPR),<sup>10,19</sup> total internal reflection fluorescence (TIRF),<sup>19</sup> and attenuated total reflectance-fourier transform infrared spectroscopy (ATR-FTIR) (Ref. 24) have been used to quantify ligand density on biomaterial surfaces. Some of these methods, like radiolabeling, are not surface sensitive and some of these methods such as SPR, TIRF, ATR-FTIR, and QCM are only applicable for ultraflat model substrates. XPS and ToF-SIMS have an information depth of  $\sim 10$  nm and  $< 5$  nm, respectively, and therefore have the correct surface sensitivity to measure surface ligands; however, it is still unclear if they have sufficient limits of detection to measure bioactive ligands at the surface densities relevant to their effect on cell attachment and behavior. Out of these methods, only radioactive labeling and XPS have a claim to absolute quantification, and only in few studies have several methods been compared and subsequently correlated with cell adhesion for a more complete picture.

In this study, we used ultrathin hydrogel films on silicon and glass surfaces functionalized with different ligands: a fluorinated amino acid and an iodinated peptide for XPS and ToF-SIMS, GRGDSK-biotin for ELISA detection and GRGDS for adhesion of HDFs. We chose the NCO-sP(EO-*stat*-PO) hydrogel coating system<sup>26</sup> as model since it is well established, may reproducibly be prepared and can be functionalized in a straightforward way by respective choice of the molar ratio between reactive prepolymer and ligand that

bears a nucleophilic chemical group. In this study, it is used as a model system for hydrogel coatings in general. Moreover, although often used and applied, surface ligand quantification has so far not been performed for this system. We functionalized the hydrogel films with ligands detectable for the different quantification methods by mixing different molar ligand to prepolymer ratios before the coating procedure. Our study shows that XPS and ToF-SIMS may be used to assess maximal ligand content that can be introduced into the hydrogel, but that this number, a molar ligand to prepolymer ratio of 1/1, does not correlate with the amount of peptide necessary at the surface to achieve maximal cell adhesion, which occurs at lower ratios of 1/5. This value may, however, be measurable by ELISA technique. Using radiolabeling, ELISA and quantitative cell adhesion as control measurements on flat substrates allowed absolute quantification of ligand densities as a standard curve for the values measured on hydrogel films.

## II. MATERIALS AND METHODS

### A. Hydrogel coating

Silicon wafer of  $1 \text{ cm}^2$  (CrysTecKristall-technologie, n-Type, Berlin, Germany) and glass slides ( $\varnothing 15$  mm, Paul Marienfeld, Lauda-Königshofen, Germany) were cleaned with isopropanol and successively cleaned in acetone, distilled water, and isopropanol in an ultrasonic bath for 5 min followed by drying in a stream of nitrogen. Solvents were purchased from Prolabo (Darmstadt, Germany). Substrates were activated by  $\text{O}_2$ -plasma treatment for 15 min (400 W, 50 sccm, and 0.4 mbar) and aminosilanized with 3-aminopropyl-trimethoxysilan at 5 mbar. NCO-sP(EO-*stat*-PO) prepolymers were synthesized as described elsewhere<sup>27</sup> and solubilized in tetrahydrofuran (THF) under inert gas atmosphere. Water was added to the NCO-sP(EO-*stat*-PO) solution (THF/ $\text{H}_2\text{O}$  1/9) to yield a final prepolymer concentration of 10 mg/ml. Five minutes after addition of water, silicon/glass slides were spin coated with the prepolymer solution filtered through a  $0.2 \mu\text{m}$  syringe filter (40 s, 2500 rpm, 5 s acceleration time).

### B. Functionalization

Ligands were solubilized in water and mixed with the NCO-sP(EO-*stat*-PO) solution in THF to a final prepolymer concentration of 10 mg/ml. For XPS and ToF-SIMS, the 4-(trifluoromethyl)-DL-phenylalanine (fluorinated amino acid) from Fluorochem (Derbyshire, England) and Ac-KRGDSP-3,5-diiodo-Y-NH<sub>2</sub> (iodinated peptide) from Bachem (Bubendorf, Switzerland) were used in ligand to prepolymer ratios of 1/2, 1/1, and 2/1. For ELISA the biotinylated peptide GRGDSK-biotin (Bachem, Bubendorf, Switzerland) was mixed-in in ratios of 1/20 to 1/1. For cell adhesion experiments, the peptide GRGDS (Bachem, Bubendorf, Switzerland) was used in molar peptide to prepolymer ratios from 1/10 to 2/1. Coatings were stored for at least 12 h at room temperature to assure complete cross linking before further usage.

### C. Radioisotopic labeling

YRGDS (Bachem, Bubendorf, Switzerland) was radiolabeled with carrier-free Na<sup>125</sup>I (NEZ0033A, PerkinElmer, Rodgau, Germany) using a modified chloramine T procedure.<sup>28</sup> YRGDS (10 μg) in 10 μg 0.4 M sodium phosphate buffer (pH 7.5) and 300 μCi Na<sup>125</sup>I were combined in a 1.5 ml plastic tube. Iodination was started by addition of 1 μg of chloramine T in 5 μl 0.04 M sodium phosphate buffer and stirred for 5 min at room temperature. After this time, another 1 μg chloramine T was added and the reaction was continued for 25 min. Subsequently, the reaction was transferred to a Sep-Pak C18 cartridge (Waters Corporation, Eschborn, Germany) that had been equilibrated with TFA/CH<sub>3</sub>CN (9/1). After washing, the radioiodinated derivative was eluted with 50% CH<sub>3</sub>CN in 0.1% TFA in fractions of 1 ml. The radiochemical purity was 99.5% by analytical reversed-phase high-performance liquid chromatography and the isolated yield of desired product was 176 μCi. Typical specific activity of the labeled peptide was between  $0.2 \times 10^{16}$  and  $2 \times 10^{16}$  cpm/mol. <sup>125</sup>I-YRGDS was stored at –20 °C in the dark until needed. Under these conditions, no radiolytic decomposition was observed. For radioisotopic measurement, coatings were washed three times with distilled water and measured in a LB 2111 Multi Crystal Gamma Counter (Berthold Technologies, Bad Wildbach, Germany).

### D. Functionalization of amine reactive 96-well plates

Fifty microliters of GRGDS or GRGDSK-biotin solution (0.2–500 μg/ml in 0.02 M Na<sub>2</sub>CO<sub>3</sub>/NaHCO<sub>3</sub>, pH 9.4) were incubated in each well of an amine reactive 96-well plate (Immobilizer™ Amine Module, Nunc, Wiesbaden, Germany) for 1 h. For radioisotopic measurements, small aliquots of radiolabeled <sup>125</sup>I-YRGDS were added to each GRGDS solution (100–1000 μg/ml in 0.02 M Na<sub>2</sub>CO<sub>3</sub>/NaHCO<sub>3</sub>, pH 9.4). Wells were rinsed three times with 1 wt. % sodium dodecylsulfate (SDS) (Bio-Rad, Munich, Germany) and three times with phosphate buffered saline (PBS) buffer. Thiofunctional poly(glycidol) (4.5 kDa, PG-SH, 13 thiol groups) was synthesized as described earlier.<sup>29</sup> For ELISA and cell experiments, plastic background of the wells was blocked by incubating 200 μl PG-SH solution (1 mM, in 0.05 M NaHCO<sub>3</sub>/NaOH, pH 11) in each well for 1 h followed by three times rinsing with distilled water. After three times washing with 2-hydroxyethylacrylat (10 mM, in 0.01 M PBS, pH 7.4, Sigma-Aldrich, Steinheim, Germany), wells were rinsed three times with distilled water. For cell experiments, wells were sterilized 20 min with UV light.

### E. Ellipsometry

For determination of coating thicknesses on silicon, a spectroscopic ellipsometer model M2000DI (J.A. Woollam Co., Lincoln, Nebraska, USA) was used with a wavelength between 195 and 1700 nm and angles of incidence of 67°, 70°, and 75°. A two parameter Cauchy model was used for the refractive index of the hydrogel films and the optical

constants for silicon and silicon oxide were taken from the database supplied by the manufacturer.

### F. XPS

Elemental composition of the surfaces of hydrogel coatings on silicon were measured with an x-ray photoelectron spectrometer model AXIS ULTRA (Kratos, Manchester, England) using a monochromatic Al K $\alpha$  x-ray source with an energy of 1486.7 eV and an angle of 60° to the surface normal. The x-ray anode was operated at a potential of 15 kV and an emission current of 15 mA (225 W). A magnetic lens was placed under the sample to efficiently collect photoelectrons into the analyzer, the average take-off angle of the electrons was normal to the surface, giving an estimated 10 nm information depth for C1s photoelectrons with kinetic energy ~1200 eV. Wide scans over the range of 200–1500 eV kinetic energy, step size 1 eV, 0.2 s per step, and pass energy 160 eV were used to identify elements present in the surface and detailed scans were performed for the C1s, O1s, N1s, F1s, and I3d<sub>5/2</sub> lines with step size 0.1 eV, 0.5 s per step, and pass energy 80 eV. For halogenated samples, a series of interlaced scans of the halogen and carbon regions were acquired prior to the wide scan to assess and account for the effects of x-ray damage. Data processing was performed using CASAXPS (Version 2.3.15). Data were transmission function corrected and background subtracted with a linear background, divided by the average matrix relative sensitivity factors and the corrected intensities normalized to the sum of all corrected intensities of the detectable elements. Under the assumption that all elements are homogeneously distributed in the sample, this provides the composition of the sample, excluding hydrogen. If there is surface excess of one or more element, then significant (>10%) errors in average composition may be made.

### G. ToF-SIMS

Secondary ion mass spectra of hydrogel surfaces on silicon were measured with a time-of-flight secondary ion mass spectrometer model TOF-SIMS IV (IONTOF, Münster, Germany). A Bi liquid metal primary ion source was used with an angle of 45° relative to the sample surface with a pulsed Bi<sub>3</sub><sup>+</sup> primary ion beam of 25 keV and rastered over fresh 100 μm × 100 μm areas for each analysis. The ToF analyzer was installed at an angle of 90° to the sample surface. Both positive and negative secondary ion spectra were collected. Mass calibration was carried out using standard procedures<sup>30</sup> (mass resolving power >5000).

### H. ELISA

ELISA protocols for use on NCO-sP(EO-*stat*-PO) coatings in well plates were developed earlier<sup>31</sup> and refined for amine reactive 96-well plates and coatings on glass for this study. Coatings on glass were placed in 24-well plates and incubated subsequently with 500 μl deionized water and 300 μl glycidol solution (2.23 mg/ml in 0.2 M bicarbonate buffer) for 60 min followed by washing three times with 300 μl PBS-Tween (0.05 vol. %, Tween-20, Roth,

Karlsruhe, Germany). The uncoated side of the substrates was blocked with 1 wt. % bovine serum albumin (BSA, Servia Electrophoresis, Heidelberg, Germany) in PBS for 60 min followed by a washing step with PBS-Tween. 200  $\mu$ l (24-well) and 50  $\mu$ l (96-well) streptavidin-peroxidase (SA-POD, 1/3000 in PBS, Roche, Mannheim, Germany) were incubated on the surfaces for 60 min and washed with PBS-Tween. After dissolving one orthophenylenediamine (OPD) tablet (Dako, Hamburg, Germany) in 6 ml deionized water and 2.5  $\mu$ l H<sub>2</sub>O<sub>2</sub> (30 vol. %), 200  $\mu$ l (24-well) and 100  $\mu$ l (96-well) of the OPD solution were added to each well. After 1 min incubation, the reaction was stopped by adding 100  $\mu$ l 3 M HCl. Optical density (OD) of each well was measured in the microplate reader model Sunrise (Tecan, Maennedorf, Switzerland) at a wavelength of 492 nm. Results are shown on a logarithmic scale. Negative control values were below 0.1.

### I. Cell culture

Primary human dermal fibroblasts (HDF, isolated from foreskin, max. passage 6) were cultured under standard cell culture conditions (37 °C, 5% CO<sub>2</sub>, 95% humidity) in Dulbecco's Modified Eagle Medium (Invitrogen Darmstadt, Germany) supplemented with 10% fetal bovine serum (Biowest, Nuaille, France) and 1% penicillin/streptomycin (PAA Laboratories, Cölbe, Germany). Coated glass substrates were placed in 24-well suspension culture plates (Greiner Bio-One, Frickenhausen, Germany) and washed thoroughly with sterile water and PBS buffer five times each. Cell suspension of 1 ml and 300  $\mu$ l (20 000 cells/ml) were seeded on each glass substrate and 96-well, respectively, and incubated under standard cell culture conditions. Additionally, cells were seeded in tissue culture polystyrene (TCPS) 24-well plates (Greiner Bio-One, Frickenhausen, Germany) as a control surface. Life cell images were taken with an Axiovert 100A imaging microscope (Carl Zeiss, Göttingen, Germany). Images of cells on glass substrates were taken after 0.25, 0.5, 1, 3, and 24 h and adherent cells counted. On functionalized 96-well plates, cells were counted after 3 h.

## III. RESULTS AND DISCUSSION

NCO-sP(EO-*stat*-PO) coatings used in this study have previously been described to minimize unspecific protein adsorption<sup>26</sup> and cell adhesion.<sup>32</sup> These coatings are prepared by spin coating of aqueous solutions of the hexa-functionalized prepolymers [Fig. 1(a)], which leads to the formation of a dense and homogeneous three-dimensional polymer network. Functionalization of the films is possible either by direct addition of the ligand of interest to the prepolymer solution or by incubation of freshly prepared coatings with the respective ligand solution.<sup>12</sup> The only prerequisite for covalent immobilization of the ligand is a nucleophilic chemical group, such as alcohols, amines, or thiols. The latter are preferred as thiols react most rapidly with isocyanates with less pH dependency than amines.

The aim of this study is to compare methods capable of detecting ligands immobilized in and on the hydrogel films and assess whether they have sufficient sensitivity to quantify the surface densities of ligands needed for the onset of proper cell adhesion. For functionalization, a fluorinated amino acid and an iodinated peptide for XPS and ToF-SIMS, GRGDSK-biotin for ELISA detection, and GRGDS for cell adhesion measurements were covalently immobilized to the NCO-sP(EO-*stat*-PO) hydrogel coatings (Figs. 1(b)–1(f)). For functionalization, all ligands were mixed with the prepolymer solution prior to spin coating in different molar ligand to prepolymer ratios. Additionally, GRGDSK-biotin, GRGDS, and <sup>125</sup>I-YRGDS were immobilized on amine reactive 96-well plates for ELISA, cell adhesion, and radioisotopic measurements.

### A. Ellipsometry

Ellipsometry measurements for determination of hydrogel coating thicknesses were important to ensure sufficient coating thicknesses for analysis with XPS and ToF-SIMS (Fig. 2). UV/O<sub>3</sub> activated silicon wafer form a layer of silicon oxide on the surface of around 2.2 nm thickness. The aminosilane layer on top of the silicon oxide layer had a thickness of 0.5  $\pm$  0.1 nm. This corresponds to approximately a monolayer of aminosilane. Hydrogel coatings on top (dry thickness of 40.7  $\pm$  5.2 nm for plain hydrogels, 25.4  $\pm$  3.5 nm for functionalized hydrogels) were sufficiently thick for XPS and ToF-SIMS analysis, so that the silicon substrate should not influence the XPS and ToF-SIMS measurements. Functionalized layers are thinner since the bound ligands lower the amount of free functional groups available for cross-linking and also affect the hydrodynamic properties, particularly in case of the fluorinated amino acid:

### B. XPS

XPS spectra demonstrated the presence of carbon, oxygen, and nitrogen at the surface of all hydrogel coatings, as expected. Additionally, fluorine was present in the case of the fluorinated amino acid and iodine in the case of the iodinated peptide. All of the samples had a trace level of silicon present in the surface which may arise from either a patchiness in the coating or from contamination. The binding energy position of  $\sim$ 102 eV indicated that silicon was in the form of siloxane rather than either silicon dioxide or metallic silicon expected from the substrate. This diagnosis was confirmed by the SIMS analysis, which identified the presence of poly(dimethylsiloxane) on the samples, hence supporting the presence of trace contamination. The XPS composition data were corrected by removal of the expected contribution from poly(dimethylsiloxane) to the carbon and oxygen intensities. Significant changes to the halogen concentrations were observed upon extended x-ray exposure, presumably due to damage from ionizing radiation, and these were accounted for using simple first order kinetic models, this is exemplified for iodine in supplementary material S1.<sup>33</sup> The extrapolated compositions prior to x-ray exposure are reported in this paper by

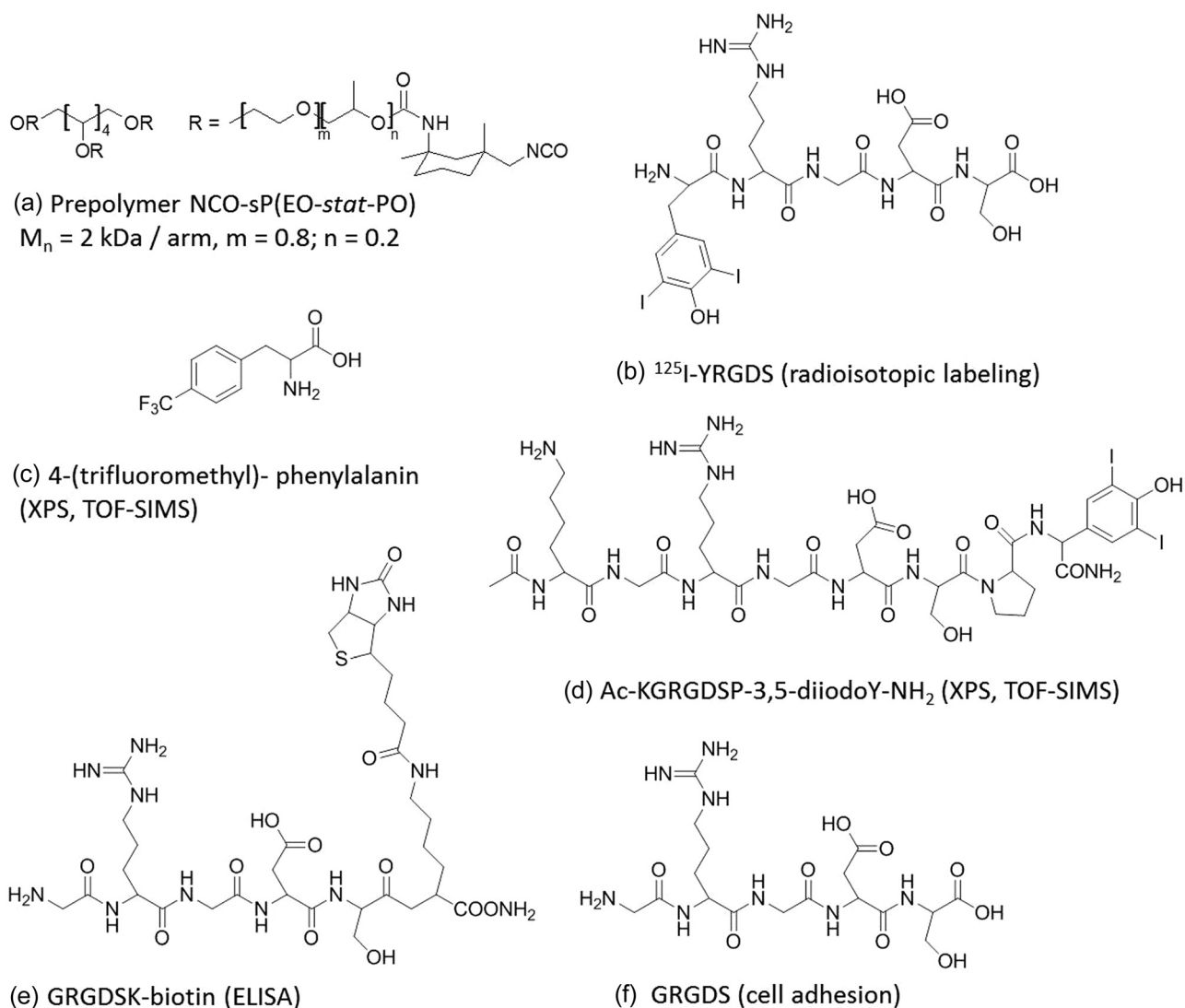


FIG. 1. NCO-sP(EO-*stat*-PO) and ligands used for functionalization. The six armed NCO-sP(EO-*stat*-PO) prepolymer (a) with a backbone of statistically copolymerized EO and PO in a ratio 4:1 and isocyanate groups at the distal endings of the polymer chains. Ligands: a fluorinated amino acid (b) and an iodinated peptide (c) for XPS and ToF-SIMS, GRGDSK-biotin (d) for ELISA detection and GRGDS (e) for cell adhesion quantification and  $^{125}\text{I}$ -YRGDS (f) for radioisotopic measurement were used for functionalization of NCO-sP(EO-*stat*-PO) hydrogels.

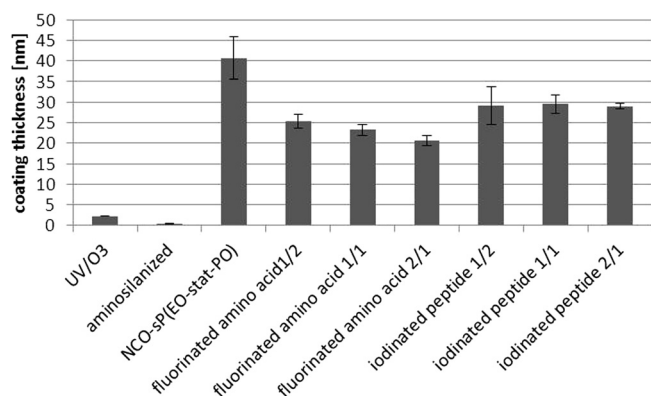


FIG. 2. Coating thicknesses of coatings determined by ellipsometry. Thicknesses of NCO-sP(EO-*stat*-PO) hydrogel coatings on silicon wafers determined by ellipsometry revealed sufficient thicknesses for XPS and ToF-SIMS measurement.

measuring the rate in change in composition and calculating the initial composition at the start of x-ray exposure. Full details of the data treatment are provided in supplementary material S2.<sup>33</sup> While the fluorinated amino acid exhibited a simple loss in fluorine with x-ray exposure, the iodine in the iodinated peptide demonstrated a transformation from organic iodide (C-I) to iodide anion ( $\text{I}^-$ ). This was evident from the shift of intensity to lower binding energy (higher kinetic energy) as shown in Fig. S1(A).<sup>33</sup> Figure S1(B) demonstrates that the capture of iodide as the anion appears to be rather efficient, but a similar effect was not observed for fluorine in the fluorinated amino acid samples.<sup>33</sup> It is possible that the presence of basic lysine and arginine groups in the peptide facilitate this capture.

Following the corrections described above, we find that the XPS compositions of carbon and oxygen for these samples are rather invariant with means and standard deviations of  $71.4 \pm 0.4 \text{ at. \% C}$  and  $26.8 \pm 0.2 \text{ at. \% O}$ . This compares

TABLE I. XPS calculations and measurements of elemental composition of coatings. Calculated and measured (gray background) trace elemental composition of pure and functionalized NCO-sP(EO-*stat*-PO) coatings with fluorinated amino acid and iodinated peptide.

Expected mole ratio	Calculated			Measured			XPS mole ratio
	N	F	I	N	F	I	
NCO-sP(EO- <i>stat</i> -PO)	1.3	0	0	1.4	0	0	
Fluorinated amino acid							
1/2	1.4	0.15	0	1.2	0.30	0	~1/1
1/1	1.4	0.30	0	1.5	0.8	0	~2.5/1
2/1	1.5	0.60	0	1.4	0.7	0	~2.3/1
Iodinated peptide							
1/2	1.9	0	0.08	1.4	0	0.02	~1/8
1/1	2.2	0	0.15	1.7	0	0.07	~1/2
2/1	3.1	0	0.30	1.7	0	0.07	~1/2

with calculated compositions of 69.0 at. % C and 29.7 at. % O for unmodified NCO-sP(EO-*stat*-PO). The variation in the concentration of nitrogen and the concentrations of halogens are rather small, and the values are given in Table I along with the expected concentrations for these modified coatings. Comparison of calculated and measured elemental composition in Table I shows that the surface concentration of ligands cannot be simply predicted from the concentration of the reaction mixtures. In the case of two iodinated peptides per prepolymer (2/1) and one iodinated peptide per prepolymer (1/1), a molar ratio of  $\sim 1/2$  was found by XPS. In case of one peptide per 2 prepolymers (1/2) even less than 50% binding efficiency was observed. Modification with the small amino acid seems more effective compared to the larger iodinated peptide. Fluorinated phenylalanine is a rather small molecule compared to the iodinated peptide containing 8 amino acids. The small amino acid may be more mobile in the prepolymer solution prior to spin coating leading to a higher binding efficiency. Additionally, the fluorinated phenylalanine is more hydrophobic, eventually making it more likely to bind to the isocyanate groups at the hydrophobic

termini of the prepolymer arms. In case of 1/2 and 1/1, the measured atom percent are significantly higher than the calculated amount assuming homogeneous distribution of the ligands throughout the coating. This may be explained by rapid binding and high mobility of the fluorinated amino acids in solution prior to spin coating so that in some cases accumulation of more than one amino acids on one prepolymer is possible. It is notable that, for both ligands, the 1/1 and 2/1 surfaces were indistinguishable in composition within the sensitivity of XPS, indicating a saturation of sites with more than equimolar mixtures of ligand to prepolymer. Furthermore, from the data acquired and the level of noise in the spectra, it is possible to estimate the limit of detection of XPS under these conditions as  $\sim 0.05\%$  for fluorine and  $\sim 0.01\%$  for iodine, which accord well with estimated detection limits for these elements in a carbon matrix.<sup>34</sup> These correspond to ligand to prepolymer molar ratios of  $\sim 1/6$  and  $\sim 1/15$ , respectively, or assuming constant composition in the analyzed volume,  $\sim 2 \times 10^{12}$  ligands/cm<sup>2</sup>. Note that this level of detection can only be achieved when there is a unique element in the ligand, preferably with a large photoionization cross section.

### C. SIMS

Pure and functionalized hydrogel coatings were analyzed with ToF-SIMS measuring negative and positive spectra. The positive secondary ion spectra showed characteristic signatures of PEO at nominal masses of  $m/z = 45, 89,$  and  $133$  Da and confirmed by their exact masses to be  $C_2H_5O^+$ ,  $C_4H_9O_2^+$ , and  $C_6H_{13}O_3^+$ .<sup>35</sup> Additionally, the presence of poly(dimethylsiloxane) contamination, indicated by XPS, on some surfaces was confirmed by characteristic secondary ions at  $m/z = 73, 147,$  and  $221$  Da. Secondary ions arising from the ligands were identified in both the positive and negative ion spectra, however the majority were either rather weak in intensity, or there were secondary ions of the same mass which arose from the substrate. The unique intense secondary ions were the fluoride ( $m/z = 19$  Da) and iodide ( $m/z = 127$  Da) anions. The intensities for these secondary ions

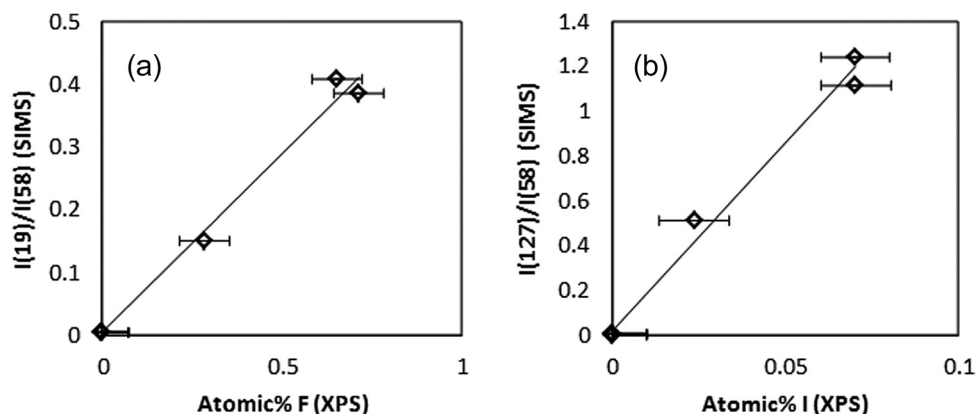


FIG. 3. Comparison of ToF-SIMS secondary ion intensity ratios to XPS compositions. ToF-SIMS data of NCO-sP(EO-*stat*-PO) all hydrogel coatings showing the correlation between the normalized halide anion secondary ion intensities and the XPS data (a) fluoride secondary ion and (b) iodide secondary ion. Lines show an unconstrained linear regression. This correlation demonstrates that calibration is possible, as has already been shown on idealized surfaces (Ref. 23).

are shown in Figs. 3(a) and 3(b), respectively, as a ratio to the  $C_2H_2O_2^-$  ( $m/z = 58$  Da) secondary ion, which is characteristic of PEO. In the dilute regime, this ratio of ligand secondary ion to polymer secondary ion should scale linearly with composition and the linear regressions shown in Fig. 3 demonstrate that this appears to be the case.

It is noteworthy that the SIMS data supports the XPS finding that the composition of the 1/1 and 2/1 samples are negligibly different. From the SIMS data, the ligand density on the 1/2 samples are slightly less than half that of the 1/1 samples, also in accord with XPS. These data suggest that the ligand density saturates for ligand/polymer reactant ratios of 1/1 or greater and at lower reactant ratios the ligand density can be controlled, although the relationship between reactant ratio and surface composition may not be straightforward. The calculated detection limit of SIMS from these data is approximately an order of magnitude better than that of XPS and therefore SIMS may be able to detect and measure ligand densities as low as  $\sim 10^{11}$  ligands/cm<sup>2</sup>, providing there are clear and unique secondary ion signals arising from the ligand.

#### D. ELISA

ELISA was used in this study as surface sensitive and bio-analog quantification method, since the protein interaction can merely take place at the hydrogel surface, and the steric restriction of protein–ligand recognition resembles the recognition of cell binding peptides by integrins. The biotinylated peptides (GRGDSK-biotin) presented at the surface of the hydrogel coating were detected using streptavidin labeled with peroxidase (SA-POD). Relative OD of the photometric detection of the product of the POD enzyme reaction is compared in Fig. 4(a). A maximal ligand concentration on the surface was reached at ligand to prepolymer ratios of 1/5 (0.2). This is in clear contrast to the XPS and ToF-SIMS measurements, which show that the overall ligand concentration does increase further when adding more ligand and saturation is reached at a ligand to prepolymer ratio of 1/1. We assign this difference to the steric constraints during ELISA, with SA-POD as rather bulky recognition molecule, in combination with the true surface sensitivity. Although ELISA is a relative method and no ligand concentrations can be extracted from these experiments, we conclude that at the surface of hydrogel films prepared with a ligand to prepolymer ratio of 5/1, the biotinylated cell adhesion peptides already form a surface concentration where a maximal density of SA-POD can be bound.

#### E. Cell adhesion

Eventually, cell adhesion is the decisive measure for biomaterials, and cell adhesion ligands are introduced into hydrogels to optimize this interaction. However, the maximal amount of ligand in a hydrogel is not necessarily the optimal ligand concentration regarding cell adhesion. Also, adhesion signals immobilized in a hydrogel might not be accessible for cell adhesion. In order to correlate the

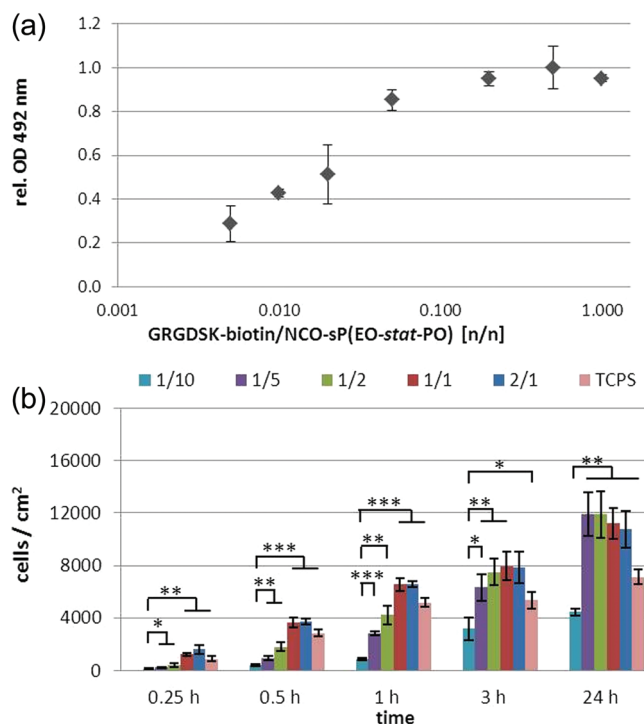
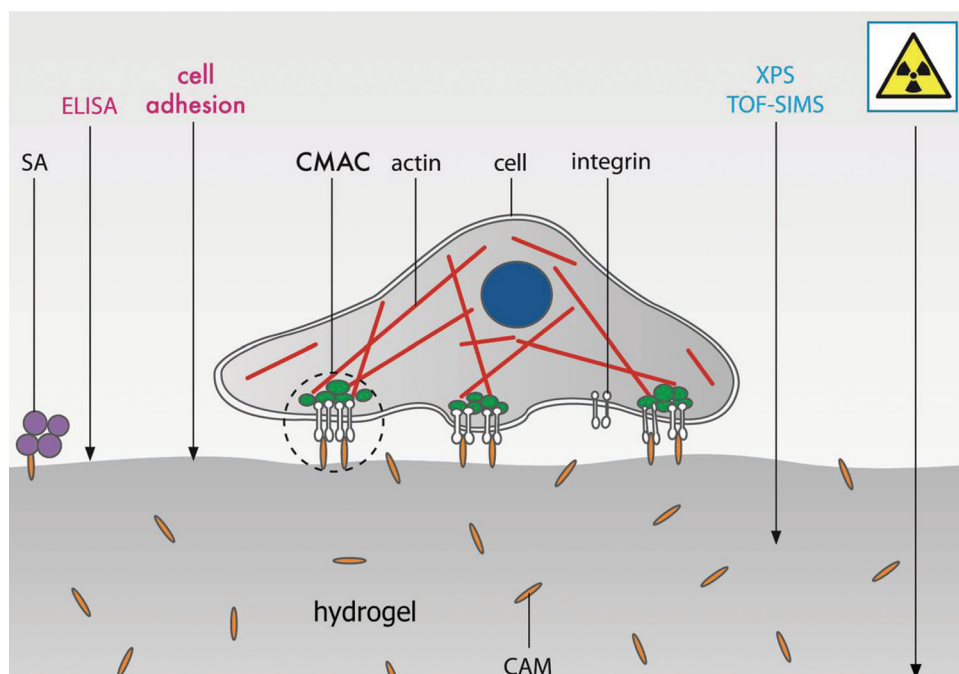


Fig. 4. ELISA and cell adhesion on functionalized hydrogel films. (a) Relative optical density of ELISA on NCO-sP(EO-stat-PO) coatings functionalized with different molar GRGDSK-biotin to prepolymer ratios. GRGDSK-biotin was detected by streptavidin-peroxidase conjugate. (b) Cell kinetic studies via life cell microscopy on NCO-sP(EO-stat-PO) coatings functionalized with different molar GRGDS to prepolymer ratios. TCPS was used as positive control for cell adhesion. Adhered cells were counted after 0.25, 0.5, 1, 3, and 24 h (\* $p < 0.05$ , \*\* $p < 0.01$ , and \*\*\* $p < 0.001$ ).

ligand quantification data presented above with cell adhesion, NCO-sP(EO-stat-PO) coatings on glass were functionalized with different amounts of the cell adhesion mediating peptide sequence GRGDS in various molar peptide to prepolymer ratios (1/10 to 2/1). Defined numbers of HDFs were cultivated on these surfaces for 24 h and cell adhesion was quantified after 15 min, 30 min, 1 h, 3 h, and 24 h [Fig. 4(b)]. Confluency was never reached in these experiments. At early timepoints up to 1 h, during initial cell adhesion, the ligand concentration has strong and significant effects on the number of adherent cells, and a higher peptide to prepolymer ratio yields in more adherent cells, up to a ratio of 1/1. Peptide fractions higher than 1/1 does not yield more adherent cells, consistent with the findings of XPS and ToF-SIMS that the surface concentration of ligands reaches a maximum at this feed ratio. Obviously, cell capture occurs more rapidly when a higher number of ligands are present. However, this effect diminishes with time. After 24 h, maximal cell adhesion was reached at peptide to prepolymer ratios of 1/5, which corresponds to the ELISA results. At this timepoint, only lower ligand concentrations (1/10) resulted in significantly lower amounts of adherent cells on the functionalized hydrogel coating surface. We suggest that, during cell capture and before proper adhesion of the cells including focal adhesion formation and cytoskeletal rearrangements, a





SCHEME 1. Overview on the different methods applied in this study for quantification of CAMs in hydrogel coatings. Even for the ultrathin ( $d < 50$  nm) layers used in this study, the hydrogels are three dimensional, and CAMs may be immobilized in the hydrogels inaccessible for cells. Therefore, classical but not strictly surface sensitive methods as well as surface sensitive methods were applied. While radiolabeling detects ligands in the bulk biomaterial, XPS and ToF-SIMS only penetrate the surface near regions depending on the experimental setup and the material characteristics. In contrast, ELISA [using streptavidin (SA)] and cell adhesion have the advantage to combine surface sensitivity and, due to the streptavidin-complex used for ELISA, exhibit a similar sterical situation, as the cell matrix adhesion contacts rely on the nanoassembly of integrins in defined geometrical constraints.

high surface ligand density favors rapid adhesion of cells. However, when given enough time and adherent cells are in an equilibrium state with respect to adhesion, an equal number of cells will become adherent also on substrates with much lower ligand concentration. These results may be explained by steric restriction in focal adhesion contacts.<sup>36</sup> Hence, the kinetics of cell adhesion can be tuned by ligand density in a much broader range than the final density of cell adhesion.

## F. Comparison of the different methods

Hydrogels, even when applied as thin and ultrathin films, are three dimensionally cross-linked multiple polymer layers. Most quantification approaches of cell adhesion on hydrogel films systems lack a comparison of different quantification methods reaching ligands in different depths of the hydrogel coatings. Scheme 1 shows a schematic overview of the different methods applied in this study and their sensitivity toward the sample surface and the steric constraints during cell-ligand interaction, and Fig. 5 summarizes the results of the sensitivities of methods used in this work and the functional behavior of the surfaces. The relationship between ligand to prepolymer feed ratio to ligand areal density is provided by the solid black line and has been derived as follows. The prepolymer shown in Fig. 1 has  $M_w$  of  $\sim 13.5$  kDa. This is approximately 1000 atoms (excluding hydrogen) with an approximate total dry volume of  $23 \text{ nm}^3$ . The cross sectional area, which will represent the average area occupied by a prepolymer at the surface, is  $\sim 8 \text{ nm}^2$ . For a 1/1 ligand/

prepolymer composition and, assuming all ligands in the surface layer of prepolymers are accessible (i.e., those within  $\sim 3$  nm of the surface), this corresponds to a ligand density of  $\sim 0.12 \text{ nm}^{-2}$ , or  $\sim 1.2 \times 10^{13} \text{ cm}^{-2}$ . Using this relationship

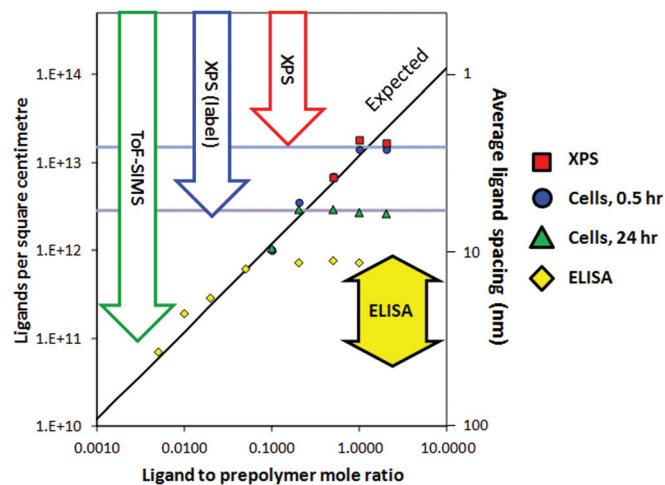


FIG. 5. Relative comparison of ligand quantification. Comparison of the methods used to assess ligand density and functional behavior of hydrogel coatings. The relationship between ligand to prepolymer feed ratio to ligand areal density is provided by the solid black line using the relationship described in detail in the manuscript text. Data from different methods are scaled so that the regions in which they are sensitive to ligand density changes align with the black line. The estimated detection limits for XPS, both with and without a unique elemental label and for SIMS are indicated by arrows and the range of ELISA by a double headed arrow. The two horizontal lines mark the maximal ligand loading achieved at a 1/1 feed ratio ( $\sim 1.5 \times 10^{13} \text{ cm}^{-2}$ ) and the minimum density of ligands to achieve constant cell density after 24 h incubation ( $\sim 3 \times 10^{12} \text{ cm}^{-2}$ ).

and assumptions, we can scale volumetric compositions to surface densities, although due to the number of assumptions the error is rather large: at least a factor of two.

Quantification by XPS and ToF-SIMS reveals a maximal ligand binding at molar ligand to prepolymer ratios of 1/1. The initial attachment of cells, after 30 min, appears to be very sensitive to ligand density over a wide range of ligand to prepolymer ratios and appears to support the conclusion from XPS and ToF-SIMS that a maximum loading of ligands occurs at molar ligand to prepolymer ratios of 1/1. The biological methods, ELISA, and cell adhesion after 24 h, reach a maximum at ratios of 1/10 and 1/5, respectively. This suggests that for adhering cells in equilibrium with fully formed adhesion contacts and cytoskeleton, the steric constraints are similar to ELISA using the HRP-SA conjugate, although ideally a slightly smaller conjugate should be employed to match the cell response. Conversion of the molar ligand to prepolymer ratios into surface densities as stated above indicates that the minimum density of ligands to achieve constant cell density after 24 h is  $\sim 3 \times 10^{12}$  ligands/cm<sup>2</sup>.

The limits of detection of the vacuum based methods can be estimated from the acquired data and indicate that XPS can only measure biologically relevant ligand densities under exceptional circumstances. However, ToF-SIMS, after suitable calibration, should be able to measure ligands at densities that span the range of importance for cell response.

### G. Quantification of surface ligand density

Unfortunately, the surface sensitive ELISA is a semi-quantitative method and allows only comparison of intensities and no determination of absolute values. Therefore, amine reactive 96-well plates were incubated with RGD peptides in different concentrations and noncovalently bound peptides were washed away with SDS and PBS. Nonfunctionalized plastic background was blocked with PG-SH, a 4.5 kDa PG containing 13 thiol groups binding flat to the plastic surface in between the RGD peptides. To ensure that no free thiols remained, wells were washed three times with 2-hydroxyethylacrylat. This resulted in true two dimensional control substrates. A maximal ELISA signal and maximal HDF adhesion were reached on surfaces incubated with peptide solutions of 50  $\mu\text{g/ml}$  [Figs. 6(a) and 6(b)]. Radioisotopic measurements reached a maximum at 741  $\mu\text{g/ml}$  [Fig. 6(c)]. With radioisotopic measurements all peptides on the surface disregarding their orientation are measured, while ELISA and cell adhesion only detect peptides accessible for SA (ELISA) and integrins in the cell membrane of HDFs and therefore orientation of the peptides influences the outcome. Additionally, an antibody and a cell cover a certain area presenting several peptides. A maximal ligand density as detected by radioisotopic measurements may therefore not be necessary for maximal ELISA signal or cell adhesion.

For quantification, we assume that for surfaces with highest detected signal, peptides do not form a dense brush like structure on the amine reactive surfaces but rather lay flat on the surface, thus occupying a space comparable to the length

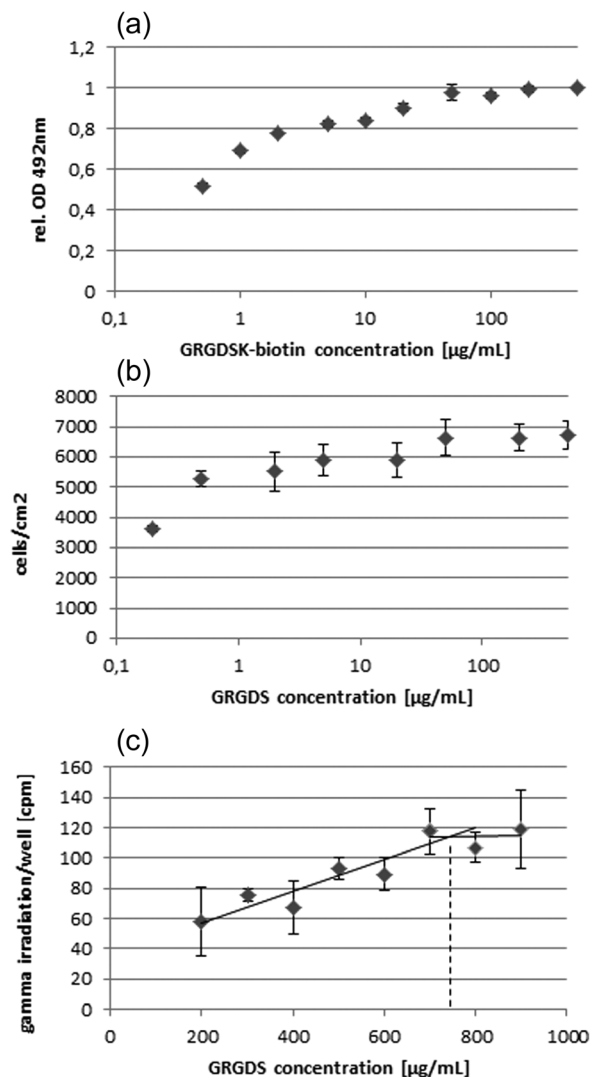


FIG. 6. Quantification of ligand density on amine reactive well plates. Amine reactive 96-well plates were functionalized with RGD peptides and were quantified using ELISA (a), cell adhesion of HDFs (b), and radioisotopic labeling (c).

of the peptide. Therefore, the peptide size diminishes the maximal possible peptide density on the amine reactive well plates. With an approximate GRGDS size of  $1 \times 2$  nm, a maximal peptide density on the surfaces of  $5 \times 10^{13}$  GRGDS/cm<sup>2</sup> is possible, which corresponds to the maximal gamma irradiation reached when incubated with GRGDS concentrations of 741  $\mu\text{g/ml}$  [Fig. 6(c)]. This peptide density is possible on amine reactive plates, which have a reactive group density of ca.  $10^{14}$  reactive groups/cm<sup>2</sup> as stated by the producer. Assuming a linear increase of GRGDS binding with increasing GRGDS concentrations, incubating 50  $\mu\text{g/ml}$  GRGDS (maximum of ELISA and cell adhesion experiments) results in a peptide density of  $4 \times 10^{12}$  GRGDS/cm<sup>2</sup>. Thus, in case of a homogeneous distribution of the peptides on the surface, these peptides are placed in an average distance of 5 nm.

For ELISA experiments another factor has to be taken into account. The tetrameric SA used for ligand detection in

ELISA experiments has a diameter of approximately 6 nm. With a dense packing of the SA on the surface in a hexagonal ordering, the diameter of the SA corresponds the distance of the centers of the SA. The theoretical maximal loading of the surface is therefore  $3 \times 10^{12}$  SA/cm<sup>2</sup>, although it is unlikely that this could be reached: the jamming limit of the random sequential adsorption model<sup>37</sup> indicates that the maximal loading could be as low as half of this value and the maximum detectable biotin density could thus be as low as  $1.5 \times 10^{12}$  ligands/cm<sup>2</sup>, with an average peptide spacing between  $\sim 5.5$  and  $\sim 8$  nm.

Due to several assumptions made in these calculations, the minimal RGD spacing on the hydrogel films can only be estimated to range between 5 and 8 nm. This is however in the range of previously detected ligand spacing using fibroblasts on RGD functionalized hydrogels.<sup>18,20</sup> Other studies on ultraflat films on hard substrates revealed different RGD spacing optimal for adhesion and spreading.<sup>36,38,39</sup> This underlines the importance of critical assessment of the amount of ligands needed for cell adhesion for each system, and the special properties of hydrogel films where obviously a higher ligand density is needed for cell adhesion than on ultraflat coatings.

#### IV. CONCLUSIONS

The aim of this study was to demonstrate the importance of comparing different quantification methods for the determination of optimal surface ligand concentrations on hydrogels for the intelligent and economic design of functional biomaterials. The optimal ligand concentrations are not necessarily maximal ligand concentrations achievable in the hydrogel system of choice, which implies that it is possible to create multifunctional materials with no loss of individual ligand function. We show that although XPS is useful to characterize surface chemistry and identify the maximum number of ligands that can be loaded into these systems, it lacks the sensitivity to measure ligand concentrations at biologically relevant levels. In contrast, ToF-SIMS is shown to have the requisite sensitivity, providing that clear and unambiguous secondary ions can be detected from the ligand and that a calibration method as indicated by the correlation shown in Fig. 4 and as shown on idealized reference surfaces<sup>23</sup> is found to convert secondary ions into surface compositions. Within this study, we found no evidence that these vacuum based methods were inconsistent with measurements performed in liquid on these materials.

Using radiolabeling, ELISA and cell adhesion on RGD-functionalized amine reactive well plates enabled the determination of a standard-curve for the signals measured on the hydrogels and allowed estimation of a minimum RGD spacing for cell proliferation of  $6.5 \pm 1.5$  nm. This value is lower than values reported for ultrathin coatings on hard surfaces, indicating the special properties of hydrogel films with their high water content and higher flexibility of the polymer chains. ELISA is sensitive to a rather narrow range of ligand densities, spanning about an order of magnitude, with an

upper limit defined by the size of the conjugate used; in this case, the upper limit is close to the minimal ligand density required for cell proliferation. The methods applied in this study are all state of the art and may readily be transferred to other hydrogel systems, and our results underline the importance of proper characterization using multiple techniques is necessary and reasonable for proper analysis of each individual system.

#### ACKNOWLEDGMENTS

The DFG (SPP 1259 Intelligent hydrogels) is acknowledged for funding. The authors thank Baron and Yvonne Marquardt (Department of Dermatology and Allergology, University Hospital of the RWTH Aachen, Germany) for providing human dermal fibroblasts. A.G.S. and S.J.S. acknowledge funding from the European Union through the European Metrology Research Programme (EMRP) project BioSurf. The EMRP is jointly funded by the EMRP participating countries within EURAMET and the European Union.

<sup>1</sup>J. M. Anderson, *Annu. Rev. Mater. Res.* **31**, 81 (2001).

<sup>2</sup>N. A. Peppas, J. Z. Hilt, A. Khademhosseini, and R. Langer, *Adv. Mater.* **18**, 1345 (2006).

<sup>3</sup>B. D. Ratner and S. J. Bryant, *Annu. Rev. Biomed. Eng.* **6**, 41 (2004).

<sup>4</sup>P. Cacciafesta, A. D. L. Humphris, K. D. Jandt, and M. J. Miles, *Langmuir* **16**, 8167 (2000).

<sup>5</sup>K. L. Prime and G. M. Whitesides, *Science* **252**, 1164 (1991).

<sup>6</sup>K. L. Prime and G. M. Whitesides, *J. Am. Chem. Soc.* **115**, 10714 (1993).

<sup>7</sup>M. Mrksich and G. M. Whitesides, *Annu. Rev. Biophys. Biomol. Struct.* **25**, 55 (1996).

<sup>8</sup>S. Herrwerth, W. Eck, S. Reinhardt, and M. Grunze, *J. Am. Chem. Soc.* **125**, 9359 (2003).

<sup>9</sup>I. Sielaff, A. Arnold, G. Godin, S. Tugulu, H. A. Klok, and K. Johnsson, *ChemBiochem* **7**, 194 (2006).

<sup>10</sup>K. Uchida, H. Otsuka, M. Kaneko, K. Kataoka, and Y. Nagasaki, *Anal. Chem.* **77**, 1075 (2005).

<sup>11</sup>L. Lavanant and H. A.: Klok, *Chimia* **62**, 793 (2008).

<sup>12</sup>P. Gasteier, A. Reska, P. Schulte, J. Salber, A. Offenhausser, M. Moeller, and J. Groll, *Macromol. Biosci.* **7**, 1010 (2007).

<sup>13</sup>S. Halstenberg, A. Panitch, S. Rizzi, H. Hall, and J. A. Hubbell, *Biomacromolecules* **3**, 710 (2002).

<sup>14</sup>Z. Zhang, S. F. Chen, and S. Y. Jiang, *Biomacromolecules* **7**, 3311 (2006).

<sup>15</sup>C. Roberts, C. S. Chen, M. Mrksich, V. Martichonok, D. E. Ingber, and G. M. Whitesides, *J. Am. Chem. Soc.* **120**, 6548 (1998).

<sup>16</sup>S. Tugulu, P. Silacci, N. Stergiopoulos, and H.-A. Klok, *Biomaterials* **28**, 2536 (2007).

<sup>17</sup>H. Shin, S. Jo, and A. G. Mikos, *Biomaterials* **24**, 4353 (2003).

<sup>18</sup>D. L. Hern and J. A. Hubbell, *J. Biomed. Mater. Res.* **39**, 266 (1998).

<sup>19</sup>T. A. Barber, G. M. Harbers, S. Park, M. Gilbert, and K. E. Healy, *Biomaterials* **26**, 6897 (2005).

<sup>20</sup>J. A. Neff, P. A. Tresco, and K. D. Caldwell, *Biomaterials* **20**, 2377 (1999).

<sup>21</sup>A. D. Cook, J. S. Hrkach, N. N. Gao, I. M. Johnson, U. B. Pajvani, S. M. Cannizzaro, and R. Langer, *J. Biomed. Mater. Res.* **35**, 513 (1997).

<sup>22</sup>S. J. Todd, D. J. Scurr, J. E. Gough, M. R. Alexander, and R. V. Uljin, *Langmuir* **25**, 7533 (2009).

<sup>23</sup>S. Ray, R. T. Steven, F. M. Green, F. Höök, B. Taskinen, V. P. Hytönen, and A. G. Shard, *Langmuir* **31**, 1921 (2015).

<sup>24</sup>U. Hersel, C. Dahmen, and H. Kessler, *Biomaterials* **24**, 4385 (2003).

<sup>25</sup>M. S. Lord, B. G. Cousins, P. J. Doherty, J. M. Whitelock, A. Simmons, R. L. Williams, and B. K. Milthorpe, *Biomaterials* **27**, 4856 (2006).

<sup>26</sup>J. Groll, T. Ameringer, J. P. Spatz, and M. Moeller, *Langmuir* **21**, 1991 (2005).

- <sup>27</sup>H. Gotz, U. Beginn, C. F. Bartelink, H. J. M. Grunbauer, and M. Moller, *Macromol. Mater. Eng.* **287**, 223 (2002).
- <sup>28</sup>W. M. Hunter and F. C. Greenwood, *Nature* **194**, 495 (1962).
- <sup>29</sup>J. Groll, S. Singh, K. Albrecht, and M. Moeller, *J. Polym. Sci. A: Polym. Chem.* **47**, 5543 (2009).
- <sup>30</sup>F. M. Green, I. S. Gilmore, and M. P. Seah, *J. Am. Soc. Mass Spectrom.* **17**, 514 (2006).
- <sup>31</sup>M. V. Beer, C. Rech, S. Diederichs, K. Hahn, K. Bruellhoff, M. Möller, L. Elling, and J. Groll, *Anal. Bioanal. Chem.* **403**, 517 (2012).
- <sup>32</sup>J. Groll, J. Fiedler, E. Engelhard, T. Ameringer, S. Tugulu, H. A. Klok, R. E. Brenner, and M. Moeller, *J. Biomed. Mater. Res.* **74A**, 607 (2005).
- <sup>33</sup>See supplementary material at <http://dx.doi.org/10.1116/1.4919015> for detailed information about XPS composition determination and change in iodine signal over time during XPS measurements.
- <sup>34</sup>A. G. Shard, *Surf. Interface Anal.* **46**, 175 (2014).
- <sup>35</sup>A. G. Shard, M. C. Davies, and E. Schacht, *Surf. Interface Anal.* **24**, 787 (1996).
- <sup>36</sup>E. A. Cavalcanti-Adam, T. Volberg, A. Micoulet, H. Kessler, B. Geiger, and J. P. Spatz, *Biophys. J.* **92**, 2964 (2007).
- <sup>37</sup>M. Rabe, D. Verdes, and S. Seeger, *Adv. Colloid Interface Sci.* **162**, 87 (2011).
- <sup>38</sup>P. D. Drumheller and J. A. Hubbell, *Anal. Biochem.* **222**, 380 (1994).
- <sup>39</sup>P. A. George, M. R. Doran, T. I. Croll, T. P. Munro, and J. J. Cooper-White, *Biomaterials* **30**, 4732 (2009).